

A Hybrid Control Development to Suppress the Noise in the Rectangular Enclosure using an Active/Passive Smart Foam Actuator

Yeung-Shik Kim^{1#}, Gi-Man Kim¹, Cheol-Ha Roh¹, C. R. Fuller²

¹ School of Mechanical Engineering, Kumoh National University of Technology, Gumi, South Korea

² Department of mechanical Engineering, Virginia Polytechnic Institute and State University, U.S.A.

Corresponding Author / E-mail: yskim@kmut.kumoh.ac.kr, TEL: +82-54-478-7346, FAX: +82-54-478-7346

KEYWORDS : Active Noise Control, Filtered-x LMS, Hybrid Control, Smart Form Actuator, Sliding Mode Control, Sliding Mode Observer

This paper presents a hybrid control algorithm for the active noise control in the rectangular enclosure using an active/passive foam actuator. The hybrid control composes of the adaptive feedforward with feedback loop in which the adaptive feedforward control uses the well-known filtered-x LMS (least mean square) algorithm and the feedback loop consists of the sliding mode controller and observer. The hybrid control has its robustness for both transient and persistent external disturbances and increases the convergence speed due to the reduced variance of the filtered-x signal by adding the feedback loop. The sliding mode control (SMC) is used to incorporate insensitivity to parameter variations and rejection of disturbances and the observer is used to get the state information in the controller design. An active/passive smart foam actuator is used to minimize noise actively using an embedded PVDF film driven by an electrical input and passively using an absorption-foam. The error path dynamics is experimentally identified in the form of the auto-regressive and moving-average using the frequency domain identification technique. Experimental results demonstrate the effectiveness of the hybrid control and the feasibility of the smart foam actuator.

Manuscript received: February 3, 2004 / Accepted: February 17, 2005

1. Introduction

There have been many research studies in the field of noise control. For the noise control there are two types of control approaches: one is the development of control algorithms and the other is the development of control techniques.

In the control algorithm, the control strategy is divided into the adaptive feedforward approach requiring reference signals and the feedback approach requiring error signals only. In the adaptive feedforward approach, Widrow *et al.*¹ first proposed the filtered-x LMS algorithm. This method is advantageous both its simplicity and the fact that error path dynamics don't have to be minimum phase system². J. V. Warner *et al.*³ applied recursive least-mean-square (RLMS) algorithm to the three-dimensional acoustic enclosure and in recent study including the filtered-x and filtered-u least-mean-square (LMS) algorithm⁴, robust performance in persistent disturbances is achieved. In the feedback approach, a modal control in the three-dimensional acoustic enclosure is introduced by Dohner *et al.*⁵. Especially in the case of a three-dimensional acoustic enclosure excited with the broadband frequency, the acoustic modes are complex and hard to control for the high frequencies, and then it needs many secondary sources for the enough noise reduction. Recently the synthesized algorithm between the adaptive feedforward and feedback control is presented, and studies show that the adaptive feedforward controller with feedback loop is effective for the vibration reduction under both transient and stationary disturbances.⁶ In this research, the feedback controller is constructed by the LQG algorithm. However, modeling errors, system uncertainties, and

disturbances are inevitable in real systems so that a robust control algorithm is necessary. The sliding mode control⁷⁻¹¹ is one of the control algorithm candidates for such systems.

In the control techniques, the active noise control^{5,6} and the active structural acoustic control^{12,13} are commonly used control techniques to minimize the noise generated by either noise sources or structural vibrations in the enclosure. Recent works^{14,15} proposed the active/passive smart form actuator as an actuator to reduce the noise and the effectiveness of its use has been investigated. The smart form is made of a porous sound-absorbing material (passive component) and a lightweight distributed PVDF film (active component). The actuator performs well at low frequency while taking advantage of the passive properties of the form at high frequency. In this paper the active/passive smart form actuator is used as actuator to reduce the noise.

The purpose of this paper is to develop the hybrid control for the effective active noise control in the enclosure using an active/passive smart form actuator. The hybrid control consists of the adaptive feedforward and the feedback loop and it has its robustness for both the transient and persistent external disturbances and increases the convergence speed due to the reduced variance of the filtered-x signal by the feedback loop effect, i.e., increment of the system damping. The well-known filtered-x LMS algorithm is used for the adaptive feedforward control and the sliding mode controller and the sliding mode observer are developed for the feedback loop. The experimental modeling technique by the state-space frequency domain identification¹⁶ is used to reduce the model order that plays a crucial role in the state feedback control design. Experiment results are

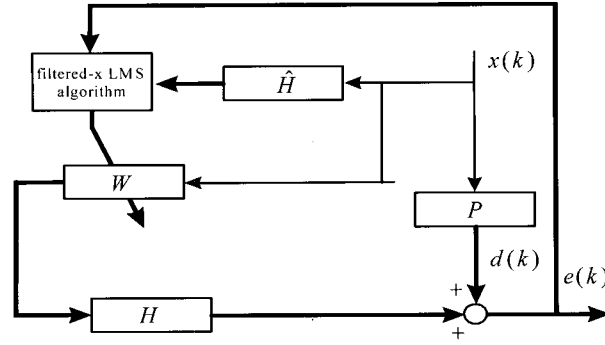


Fig. 1 Filtered-x LMS algorithm

presented for the verification of the proposed approach and show the effective reduction of the noise label under Gaussian random external disturbances.

2. DESIGN OF HYBRID CONTROL SYSTEM

Modeling the systems theoretically is generally very difficult or sometimes impossible to the complex systems. Therefore, the experimental modeling technique by the state-space frequency domain identification is introduced for the accurate model of complex shaped structures. This approach is much free from the model order problem caused in the controller design and the digital implementation comparing with the other experimental identification techniques.

Now, let us consider a general linear system of r inputs and m outputs. By the state-space frequency domain identification, the transfer function of the system in z -plane can be represented as follows:

$$x(k+1) = Ax(k) + Bu(k), \quad y(k) = Cx(k) + Du(k) \quad (1)$$

where $x(k)$ are states, $y(k)$ are output of the system, $u(k)$ are inputs, and $A, B, C,$ and D are system matrices respectively.

2.1 Adaptive Feedforward Control

Let us derive the multiple filtered-x LMS algorithm. Figure 1 represents the block diagram of the multiple filtered-x LMS algorithm. The error signal $e_n(k)$ at the n -th sensor is the sum of the disturbance and the secondary source signals. The error path dynamics is represented by the finite impulse response (FIR) of the order p , i.e., $h_n = [h_n(0), h_n(1), \dots, h_n(p)]^T$. The FIR filter of the order q also represents the adaptive controller, which is $w_k = [w_k(0), w_k(1), \dots, w_k(q)]^T$ where subscript k denotes the time step at which the filter coefficients are updated. The n -th error signal at the k -th step is as follows,

$$e_n(k) = d_n(k) - \sum_{m=1}^M \sum_{j=0}^q \sum_{i=0}^p h_{nm}(j) w_{m,k-j}(i) x(k-j-i) \quad (2)$$

where $d_n(k)$ is the noise signal induced by the external disturbance.

One of the optimal adaptive algorithms, the gradient descent method, is applied to find the global minimum value of the cost function $J = \sum e_n^2$ under the assumption that the coefficients of the controller are slowly changing.

$$\begin{aligned} w_{m,k+1}(i) &= w_{m,k}(i) + 2\mu(q+1) \sum_{n=1}^N e_n(k) \sum_{j=0}^q h_{nm}(j) x(k-j-i) \\ &= w_{m,k}(i) + 2\mu(q+1) \sum_{n=1}^N e_n(k) f_{nm}(k-i) \end{aligned} \quad (3)$$

Where μ is the convergence coefficient and $w_{m,k}(i)$ is the i -th coefficient of the m -th controller at the k -th sampling. This is the multiple filtered-x LMS algorithm having one reference input and the multiple error path dynamics. f_{nm} is the filtered-x signal, which is obtained by passing the reference input through the error plant H_{nm} .

$$f_{nm}(k-i) = \sum_{j=0}^p h_{nm}(j) x(k-j-i) \quad (4)$$

Now, let us move onto the reason of inserting the feedback loop into adaptive feedforward controller. By applying Lyapunov stability criterion for the SISO case for the simple deduction, the new convergence coefficient η is determined as follows,⁹

$$0 < \eta < \frac{1}{\sum_{i=0}^q f^2(k-i)} \quad (5)$$

where η equals to $\mu(q+1)$. After the coefficient of adaptive controller is converged, the filtered-x signal may be assumed with variance σ_f^2 if q external disturbance is under stationary random process. Since $\sum f^2(k-i)$ of equation (5) is equal to $(q+1)\sigma_f^2$ or $\text{Tr}(R_f)$ for the active control process under such a condition, equation (5) is identical with the stability criterion of iterative steepest descent algorithm. $\text{Tr}(R_f)$ denotes the trace of auto-covariance matrix of filtered-x signal. Equation (5) means that convergence coefficient of filtered-x LMS algorithm should be set inverse proportionally to the magnitude of filtered-x signal or impulse response of error plant H_{nm} . Therefore if external disturbance were consisted of the frequency components near to resonance of the error plant, feedforward controller adapted by filtered-x LMS algorithm would converge very slowly and be unsuitable for the control of frequently changing external disturbance.

In order to increase the convergence speed of the adaptive feedforward controller, a feedback controller may be used to improve the dynamics of error plant, such as increasing the damping capacity. This is the basic idea of proposed algorithm related with the design of hybrid controller. Note that when feedforward controller is combined with feedback loop, feedforward controller should be adapted based on the other filtered-x signal which is estimated using closed-loop transfer function $C = (I - HG)^{-1}H$ instead of error plant H . Equation (5) can be converted into the adaptation rule for multiple feedforward controllers with feedback loop,

$$w_{m,k+1}(i) = w_{m,k}(i) + 2\gamma \sum_{n=1}^N e_n(k) \sum_{j=0}^{p'} c_{nm}(j) x(k-j-i) \quad (6)$$

where FIR filter of p' order, $[c_{nm}(0), c_{nm}(1), \dots, c_{nm}(p')]^T$ is impulse response weights of transfer function between m -th feedforward control signal and n -th residual vibration, namely the closed-loop transfer function C_{nm} . Note that impulse response weights $[c_{nm}(0), c_{nm}(1), \dots, c_{nm}(p')]^T$ can be significantly less than ones of error plant $[h_{nm}(0), h_{nm}(1), \dots, h_{nm}(p)]^T$ if feedback loop

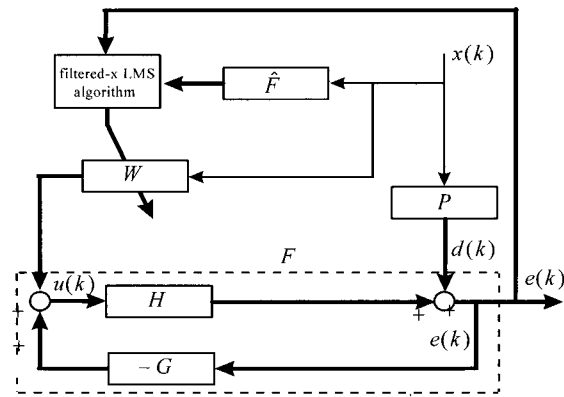


Fig. 2 Hybrid control

increases the damping capacity of secondary plant, and so convergence coefficient of the proposed algorithm γ can be set more greatly than η . Therefore, hybrid active controller may be able to attenuate even transient external disturbance as illustrated in later section by numerical simulation. Additionally, calculation burden for updating hybrid controller may be reduced because of $p' < p$.

2.2 State Feedback Control

The block diagram of hybrid control constructed by the multiple adaptive feedforward control with feedback loop is shown in Figure 2. In the feedback control of the error path, the sliding mode controller and observer are applied to the discrete error path model.

2.2.1 Sliding Mode Controller

Consider the n th order linear time invariant system (equation (1)) with m inputs given by

$$x(k+1) = Ax(k) + Bu(k) \quad (7)$$

where $\text{rank}(A)=n$ and $\text{rank}(B)=m$. Define a switching function $s(k)$ as

$$s(k) = Sx(k) \quad (8)$$

Where $S \in R^{m \times n}$ is of full rank and the hyperplane defined as $S = \{x(k) \in R^n : s(k) = 0\}$. By defining an orthogonal $T_r \in R^{n \times n}$ and the new coordinates as $z(k) = T_r x(k)$, then each equation (7) and (8) can be expressed in regular form

$$\begin{aligned} z_1(k+1) &= A_{11}z_1(k) + A_{12}z_2(k) \\ z_2(k+1) &= A_{21}z_1(k) + A_{22}z_2(k) + B_2u(k) \end{aligned} \quad (9)$$

$$s(k) = S_1z_1(k) + S_2z_2(k) \quad (10)$$

From the relationship between equations (7)-(8) and equations (9)-(10), following relationships can be obtained as

$$T_r A T_r^T = \begin{bmatrix} A_{11} & A_{12} \\ A_{21} & A_{22} \end{bmatrix}, \quad T_r B = \begin{bmatrix} 0 \\ B_2 \end{bmatrix} \quad (11)$$

Suppose at time $k = k_s$, the system states lie on the surface S and an ideal sliding motion takes place. This can be expressed mathematically as $s(k) = 0$, i.e. $S_1z_1(k) + S_2z_2(k) = 0$ for all $k \geq k_s$. On the sliding surface the equation is re-expressed as

$$z_2(k) = -S_2^{-1}S_1z_1(k) = -Mz_1(k) \quad (12)$$

where $M = -S_2^{-1}S_1$. On the sliding surface combining equation (10) with equation (9), the regular form is expressed as

$$z_1(k+1) = (A_{11} - A_{12}M)z_1(k) \quad (13)$$

The problem of hyperplane design may be considered to be a state feedback problem for the system where $z_2(k)$ is considered to play the role of the control action. In the context of designing a regulator, the matrix governing the sliding motion ($A_{11} - A_{12}M$) must have stable eigenvalues. It should be noted that, whichever scheme is chosen, fixing M does not uniquely determine S since there are m^2 degrees of freedom in the relationship

$$S_2M = S_1 \quad (14)$$

The hyperplane matrix S will be determined from M simply letting $S_2 = I_m$, giving

$$S T_r^T = [M \quad I_m] \quad (15)$$

To determine the switching hyperplane S , the quadratic performance index is defined as

$$J = \frac{1}{2} \sum_{k=k_s}^{\infty} x^T(k) Q x(k) \quad (16)$$

where Q is both symmetric and positive definite and k_s is the time at which the sliding motion commences, and Q is performed coordinate transformation.

$$T_r Q T_r^T = \begin{bmatrix} Q_{11} & Q_{12} \\ Q_{21} & Q_{22} \end{bmatrix} \quad (17)$$

By defining the optimal problem associated with constraint equation (9) and performance index equation (16), the algebraic matrix Riccati equation^[7] are derived with coordinate transformation as

$$P_1 \tilde{A} + \tilde{A}^T P_1 - P_1 A_{12} Q_{22}^{-1} A_{12}^T P_1 + \tilde{Q} = 0 \quad (18)$$

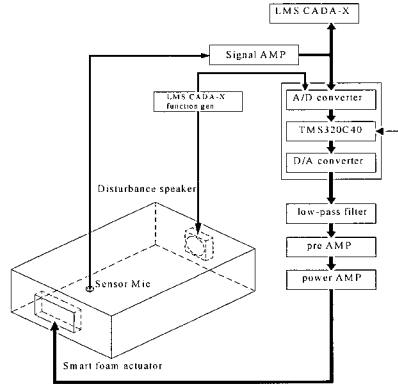


Fig. 3 (a) Experimental setup-block diagram

Where P_1 is positive definite and $\tilde{A} = A_{11} - A_{12}Q_{22}^{-1}Q_{21}$. From the unique solution of Riccati equation (P_1), M defined in equation (12) can be expressed as

$$M = -Q_{22}^{-1}(A_{12}^T P_1 + Q_{21}) \quad (19)$$

Therefore, the hyperplane S can be designed from equation (15). For the sliding mode controller design, consider a system equation with known uncertainty, f

$$x(k+1) = Ax(k) + Bu(k) + f(t, x, u) \quad (20)$$

$$f(t, x, u) = B\xi(t, x, u) \quad (21)$$

where ξ presents uncertainties or nonlinearities. SMC⁷ has two part, linear feedback component (u_l) and nonlinear feedback component (u_n). The SMC law can be expressed as

$$u(k) = u_l(k) + u_n(k) \quad (22)$$

where,

$$u_l(k) = -\Lambda^{-1}(SA - \Phi S)x(k) \quad (23)$$

$$u_n(k) = -(\eta \|\Lambda\|^{-1} \|s(k)\| + \beta)f(s(k))$$

$$f(s(k)) = \frac{s(k)}{|s(k)| + \delta} \quad (24)$$

where $\Lambda = SB$, η is positive scalar, β is model uncertainties, and Φ is eigenvalue of the switching function which makes chattering amplitude lower and reaching time to the sliding surface faster. $f(s)$ is a signum function and the slope of the signum function depends on δ .

2.2.2 Sliding mode observer

Consider the system equation (1) with system uncertainties as

$$\begin{aligned} x(k+1) &= Ax(k) + Bu(k) + f(k, x, u) \\ y(k) &= Cx(k) + Du(k) \end{aligned} \quad (25)$$

The problem to be considered involves estimation the states of the uncertain system given in equation (25) so that the error system

$e(k) = \hat{x}(k) - x(k)$ is quadratically stable despite the presence of the uncertainty. Now consider a Walcott and Żak¹⁰ observer with the following assumption. There exists an output feedback gain matrix $L \in R^{n \times p}$ such that $A_0 = A - LC$ has stable eigenvalues and there exists a Lyapunov matrix P satisfying

$$PA_0 + A_0^T P = -Q \quad (26)$$

for some positive definite matrix Q and the structural constraint

$$C^T F^T = PB \quad (27)$$

is satisfied for some $F \in R^{m \times p}$. Utilizing this assumption, an observer of the form is expressed as

$$\hat{x}(k+1) = A_0 \hat{x}(k) - LCe(k) + M(\hat{x}, y, \rho) + Bu(k) \quad (28)$$

$$M(\hat{x}, y, \rho) = \begin{cases} -\frac{BFCe(k)}{\|FCE(k)\|} \rho, & \|FCE(k)\| \geq \varepsilon_0 \\ -\frac{BFCe(k)}{\varepsilon_0} \rho, & \|FCE(k)\| < \varepsilon_0 \end{cases} \quad (29)$$

where ρ is the known boundary scalar function, and ε_0 depends on the error radius.

3. EXPERIMENTAL RESULTS

Figure 3 shows the experimental setup. The acoustic rectangular enclosure has the inner dimension of $150 \times 100 \times 40$ (cm) and is surrounded by the composite barrier composed a sandwich of two sheets of wood plate with a middle layer of sand in order to eliminate the complex structure-borne sound radiation. According to this inner enclosure size, the natural frequencies of (1, 0, 0), (0, 1, 0), and (1, 1, 0) modes are theoretically 114.3Hz, 171.5Hz, and 206.1Hz, respectively. For the noise reduction in the rectangular enclosure, the error microphone is placed as shown in the top view in Figure 3. In experimental modeling process, LMS CADA-X with Scadas II front-end and DI-2200 FFT analyzer are used for the frequency domain identification using the Gaussian random signal of the band of 80~250Hz and the evaluation of the developed control system. The hybrid control algorithm is embodied using digital signal processing unit (Loughborough, TMS320C40 DSP) with sampling rate of 2K Hz. In the modeling process of the error path dynamics including, power amplifier, a smart form actuator, acoustic characteristics in the

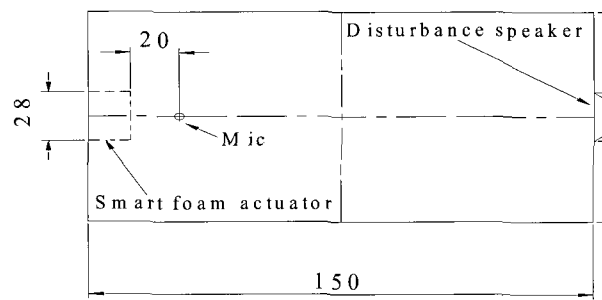


Fig. 3 (b) Experimental setup-location of actuator, microphone, and disturbance (cm)

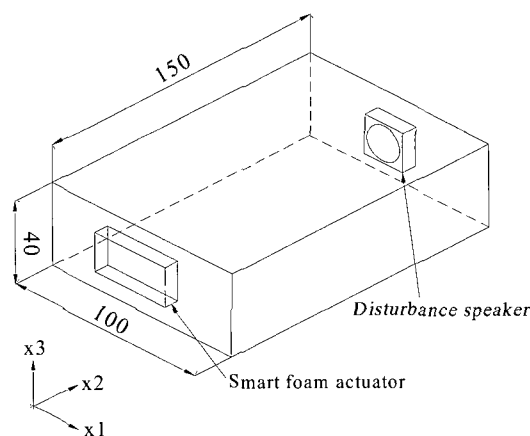


Fig. 3 (c) Experimental setup-three dimensional view of the system

enclosure, error microphone (Han-umpa, ECM101), and signal amplifiers, the system model is experimentally identified in the form of the Auto-Regressive Moving-Average (ARMA) in the frequency domain using frequency responses. Even though FIR filter coefficients of the Moving-Average (MA) model of the controlled error path are downloaded to the DSP unit, the ARMA model is needed for the feedback controller design. The frequency domain identification procedure is described briefly. First, determine frequency responses from input and output data sequences. Second, curve fit the frequency response function using the matrix fraction description method. Third, conduct minimum realization, which cancels matched poles and zeros within a tolerance. Fourth, conduct another realization, balanced realization, which algorithm finds a realization having equal and diagonal controllability and observability gramians. In this study a frequency response of an error path for single-input-single-output model is measured using FFT analyzer, and after following the above procedures, the model order is determined as 12.

Figure 4 shows comparison between the measured and modeled frequency responses. The frequency response of 80–250Hz is used for the calculation. The measured natural frequencies of modes (1, 0, 0), (0, 1, 0) and (1, 1, 0) are 111.0Hz, 193.0Hz, and 222.0Hz, respectively. It is observed that in the transfer function each modes (1, 0, 0), (0, 1, 0) and (1, 1, 0) has similar magnitude since the error microphone placed close to the smart foam actuator. The error path is controlled using the sliding mode controller and observer. Since the

model order was 12, 12 switching functions are defined to control each state. Since the model order is critical in the feedback controller design, the model order needs to be minimized within the realm of possibility.

Figure 5 represents the error path dynamics between the modeled system and the feedback-controlled system. This frequency response is just used as a criterion in the controller and observer gains design. The frequency response of the sliding mode control system is obtained from input-output data in the system.

Figure 6 shows spectrums at the error microphone with three different control approaches. In the *filtered-x LMS* algorithm the convergence coefficient η used was 0.02. In this figure, the hybrid control shows robustness to the transient and persistent external disturbances, and increases the convergence speed due to the *reduced variance of the filtered-x signal by the feedback loop effect*, i.e., increment of the system damping. It is observed that the disturbance dynamics is damped about 6dB by feedback loop. When the hybrid control starts, about 11dB reduction for $\eta=0.05$ is obtained. This figure also shows that the smart form actuator is effective for active noise control at low frequency in the enclosure with the proposed control algorithm. The passive property of the smart form at high frequency is not discussed in this paper since it was already discussed and verified in the papers^{14,15}.

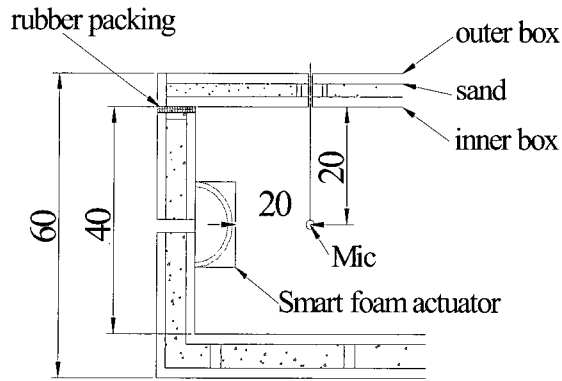


Fig. 3 (d) Experimental setup-details of the enclosure structure (cm)

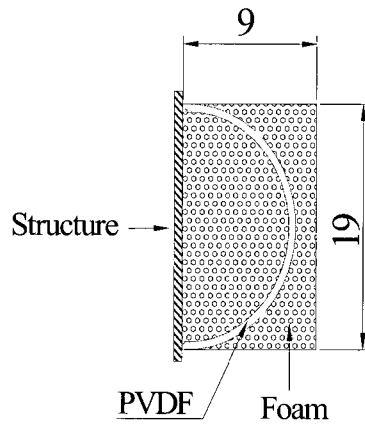


Fig. 3 (e) Experimental setup- size of smart foam (cm)

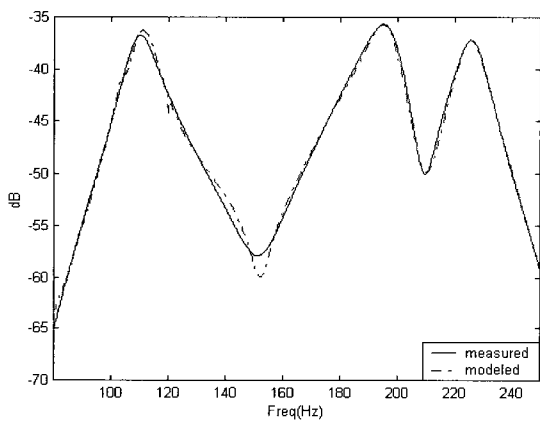


Fig. 4(a) Identification results of error path (Magnitude)

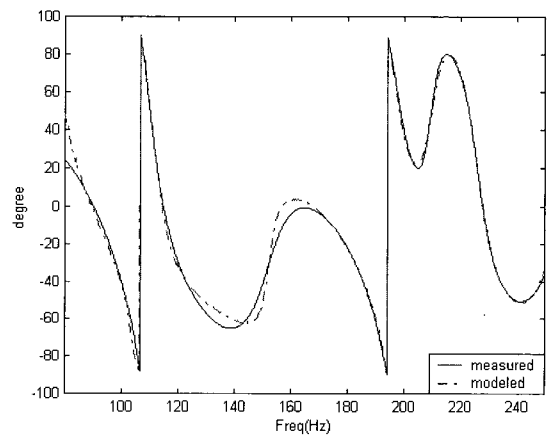


Fig. 4 (b) Identification results of error path (Phase)

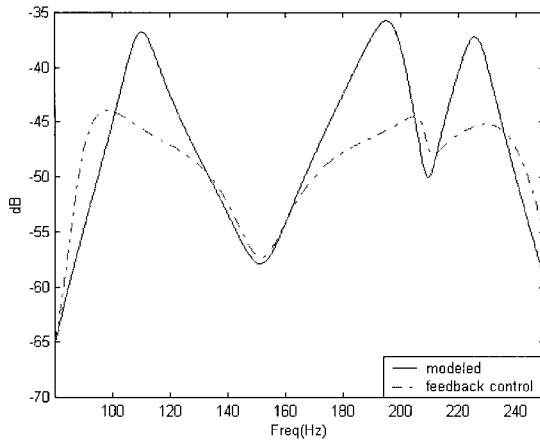


Fig. 5 Error path dynamics with feedback loop

4. CONCLUSIONS

The hybrid control, an adaptive feedforward controller with feedback loop, has been developed for the noise suppression in the acoustic rectangular enclosure using an active/passive smart form actuator. The *filtered-x LMS* algorithm is adopted in the adaptive feedforward control and the sliding mode controller and the sliding mode observer are developed for the feedback loop. In the error path dynamics, adding damping to the error path by the feedback loop makes the convergence time be short and the resultant controller is robust to transient and persistent external disturbance. Experiment results are examined the validity of the proposed approach and show the effectiveness of an active/passive smart form actuator for the noise reduction under Gaussian random external disturbances. With developed control algorithm about 11dB suppression of the noise across the first three modes of 80~250Hz in the rectangular enclosure is accomplished.

ACKNOWLEDGEMENT

This research work is conducted under the support of 2002 Research Fund of the Kumoh National University of Technology. The authors gratefully acknowledge the comments, supplying the smart form skin and help of Profs. C. R. Fuller and M. Johnson, Virginia Polytechnic Institute and State University.

References

1. Widrow B. and Stearns, S. D., *Adaptive Signal Processing*, Prentice Hall, 1985.
2. Ren, Wei and Kumar, P. R., "Adaptive Active Noise Control: Structures, Algorithms and Convergence Analysis," *Inter-Noise*, Newport Beach, CA, USA, pp. 435-440, 1989.
3. Warner, J. V. and Bernhard, R. J., "Digital Control of Sound Fields in Three-dimensional Enclosure," *AIAA 11th Aeroacoustics Conference - Palo Alto, California*, 1987.
4. Nelson, P. A. and Elliott, S. J., "Active control of sound," Academic Press, 1992.
5. Dohner, J. L. and Shoureshi, R., "Modal Control of Acoustic Plants," *ASME, J. of Dynamic Systems, Measurement and Control*, Vol. 111, pp. 326-330, 1989

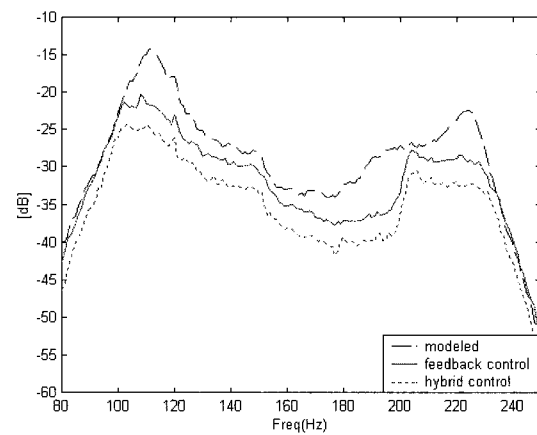


Fig. 6 Power spectrums at a microphone sensor

6. Kim, Y. S., Kim, I. S. and Lee, C., "Active Noise Control in the Acoustic Rectangular Enclosure using Multiple Adaptive Feedforward Control with Feedback Loop," *The Fourth International Conference on Motion and Vibration Control*, pp. 467-472, 1988.
7. Edwards, Christopher & Spurgeon, Sarah K., "Sliding Mode Control: Theory and Application," Taylor & Francis, 1998.
8. Young, K. D., Utkin, V. I. and *Üzgiiner, Ü.*, "A Control Engineering's Guide to Sliding Mode Control," *IEEE Transaction on Control Systems Technology*, Vol. 7, No. 3, May 1999.
9. Utkin, V. I., "Sliding Modes in Control Optimization," Springer Vellag, Berlin, 1992.
10. Walcott, B. L. and Zak, S. H., "Observation of dynamical systems in the presence of bounded nonlinearities/uncertainties," *In Proceedings of the 25. Conference on Decision and Control*, pp. 961-966, 1986.
11. Walcott, B.L. and Zak, S.H., "State observation of nonlinear uncertain dynamical systems," *IEEE Transaction on Automatic Control*, 32, pp. 166-170, 1987.
12. Fuller, C. R., Hansen, C. H. and Snyder, S. D., "Experimental on Active Control of Sound Radiation from a Panel Using a Piezoceramic Actuator," *J. of Sound and Vibration*, 150(2), pp. 179-190, 1991.
13. Sun, J. Q., Norris, M. A., Rossetti, D. J. and Highfill, J. H., "Distributed Piezoelectric Actuators for Shell Interior Noise Control," *ASME J. of Vibration and Acoustics*, Vol. 118, pp. 676-681, 1996.
14. Guigou, C. and Fuller, C. R., "Control of Aircraft Interior Broadband Noise with form-PVDF Smart Skin," *J. of Sound Vibration*, Vol. 220(3), pp. 54-557, 1999.
15. Johnson, B. D. and Fuller, C. R. "Broadband Control of Plate Radiation using a Piezoelectric, Double-amplifier Active-skin and Structural Acoustic Sensing," *J. Acoustical Society of America*, 107(2), pp. 876-884, 2000.
16. Juang, Jer-Nan *Applied System Identification*, Prentice Hall, 1994.